Comparative Molecular Field Analysis of in Vitro Growth Inhibition of L1210 and HCT-8 Cells by Some Pyrazoloacridines

Jerome P. Horwitz,*,† Irina Massova,† Thomas E. Wiese,‡ Antoinette J. Wozniak,† Thomas H. Corbett,† Judith S. Sebolt-Leopold,§ David B. Capps,§ and Wilbur R. Leopold§

Division of Hematology/Oncology, Departments of Internal Medicine and Biochemistry, Wayne State University School of Medicine, Detroit, Michigan 48202, and Parke-Davis Pharmaceutical Research, Division of Warner-Lambert Company, Ann Arbor, Michigan 48105

Received May 7, 1993•

In vitro screening of a number of 2-(aminoalkyl)-5-nitropyrazolo[3,4,5-*kl*]acridines has previously indicated (Sebolt, J. S.; et al. *Cancer Res.* **1987**, *47*, 4299–4304) that these compounds, in general, exhibit selective cytotoxicity against the human colon adenocarcinoma, HCT-8, cell line, relative to mouse leukemia L1210 cells. Comparative molecular field analysis (CoMFA) was applied to HCT-8 and L1210 growth inhibition assays (IC_{50s}) of a series (44) of the pyrazoloacridine derivatives with the objective of predicting improved solid tumor selectivity. In the absence of crystallographic data, the 9-methoxy derivative (**15**), which is currently in clinical study, was selected as the template molecular model. Two different structural alignments were tested: an alignment of structures based on root mean square (RMS)-fitting of each structure to **15** was compared with an alternative strategy, steric and electrostatic alignment (SEAL). Somewhat better predictive cross-validation correlations (r^2) were obtained with models based on RMS vis-à-vis SEAL alignment for both sets of assays. A large change in lattice spacing, e.g., 2 to 1 Å, causes significant variations in the CoMFA results. A shift in the lattice of half of its spacing had a much smaller effect on the CoMFA data for a lattice of 1 Å than one of 2 Å. The relative contribution of steric and electrostatic fields to both models were about equal, underscoring the importance of both terms. Neither calculated log *P* nor HOMO and/or LUMO energies contribute to the model. Steric and electrostatic fields of the pyrazoloacridines are the sole relevant descriptors to the structure–activity (cross-validated and conventional) correlations obtained with the cytotoxic data for both the L1210 and HCT-8 cell lines. The cross-validated r^2, derived from partial least-squares calculations, indicated considerable predictive capacity for growth inhibition of both the leukemia and solid-tumor data. Evidence for the predictive performance of the CoMFA-derived models is provided in the form of plots of actual vs predicted growth inhibition of L1210 and HCT-8 cells, respectively, by the pyrazoloacridines. The steric and electrostatic features of the QSAR are presented in the form of standard deviation coefficient contour maps of steric and electrostatic fields. The maps indicate that increases or decreases in steric bulk that would enhance growth inhibition of HCT-8 cells would likewise promote growth inhibition of L1210 cells. Contour maps generated to analyze the electrostatic field contributions of the pyrazoloacridines to growth inhibition provide an essentially similar set of results. It is apparent that steric and electrostatic fields alone are inadequate in the CoMFA to characterize the in vitro solid tumor selectivity of the pyrazoloacridines. This points to a need to supplement the cytotoxic data with results of further study that focuses on a quantitative comparison of the potential for differential metabolic activation of the pyrazoloacridines in the two cell lines.

Introduction

Sebolt and co-workers discovered that 9-methoxy-*N*,*N*-dimethyl-5-nitropyrazolo[3,4,5-*kl*]acridine-2(6*H*)-propanamine (Table I, **15**) was one of several related pyrazoloacridines to exhibit selective cytotoxicity for human colon adenocarcinoma HCT-8 cells compared to murine L1210 leukemia cells.[1a,b] In this study, which covered a wide series of 2-(aminoalkyl)-5-nitropyrazolo[3,4,5-*kl*]acridines (Table I, **1**–**44**), tissue culture growth inhibition assays demonstrated that 29 of 46 compounds tested (63%) were more active against the HCT-8 line. When compared to the several 9-alkoxy-substituted compounds in the series, the 9-methoxy derivative, **15**, proved to be superior in its activity against a panel of human and murine tumor cell lines relative to its activity against both human and murine leukemia cells.[1a] Interestingly, HCT-8 appeared to be the most sensitive cell line in the panel.

During the same time period, Wozniak observed that **15** exhibited selective cytotoxicity for solid tumor pancreatic and colon cells of the mouse, compared to leukemia cells in a soft agar disk diffusion assay.[2] Moreover, this compound proved to be highly active against several transplantable murine solid tumors.[2,3] In vivo, this agent was curative against colon adenocarcinoma 38 and pancreatic ductal adenocarcinoma 03, a finding consistent with the cellular cytotoxicity seen for this agent in the disk diffusion assay.[2] On the basis of these and subsequent findings (vide infra), **15** has been selected for phase I clinical investigation.

The pyrazoloacridines, as might be expected, intercalate into DNA, based on measurements of the displacement of ethidium from DNA.[3b] Like other intercalating agents,

† Division of Hematology/Oncology, Department of Internal Medicine.
‡ Department of Biochemistry.
§ Parke-Davis Pharmaceutical Research Division.
• Abstract published in *Advance ACS Abstracts*, October 1, 1993.

0022-2623/93/1836-3511$04.00/0

Table I. Growth Inhibition of L1210 and HCT-8 Cells by Some Pyrazoloacridines

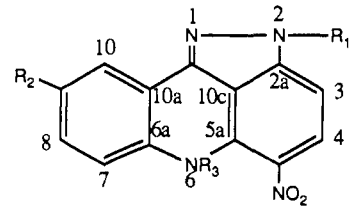

compd	R_1	R_2	R_3	IC_{50} (μM)[a] L1210	IC_{50} (μM)[a] HCT-8
1	$(CH_2)_3NMe_2$	AcO	H	0.001	0.011
2	$(CH_2)_3NMe_2$	HO	H	0.002	0.012
3	$(CH_2)_2NEt_2$	HO	H	0.002	0.013
4	$(CH_2)_2NEt_2$	AcO	H	0.004	0.005
5	$(CH_2)_2NEt_2$	$Me_3CSi(Me_2)O$	H	0.006	0.006
6	$(CH_2)_3NMe_2$	$Me_3CC(O)O$	H	0.008	0.027
7	$(CH_2)_2NEt_2$	$Me_cC(O)O$	H	0.010	0.010
8	$(CH_2)_2NEt_2$	H	H	0.192	0.185
9	$(CH_2)_2NHEt$	MeO	H	0.208	0.124
10	$(CH_2)_2NH(CH_2)_2OH$	H	H	0.218	0.152
11	$(CH_2)_3NMe_2$	EtO	H	0.220	0.055
12	$(CH_2)_2NMe_2$	EtO	H	0.275	0.025
13	$(CH_2)_2NH(CH_2)_2OH$	EtO	H	0.325	0.082
14	$(CH_2)_2NMe_2$	MeO	H	0.396	0.105
15	$(CH_2)_3NMe_2$	MeO	H	0.424	0.136
16	$(CH_2)_2NH(CH_2)_2OH$	MeO	H	0.450	0.193
17	$(CH_2)_2NEt_2$	MeO	H	0.469	0.123
18	$(CH_2)_2NEt_2$	PrO	H	0.469	0.031
19	$(CH_2)_2NH(CH_2)_2OH$	H	Me	0.510	0.518
20	$(CH_2)_3NMe_2$	MeS	H	0.513	0.352
21	$(CH_2)_2NH(CH_2)_2OH$	Me	H	0.592	0.255
22	$(CH_2)_2NMe_2$	Me_2N	H	0.601	0.164
23	$(CH_2)_2NEt_2$	MeO	Me	0.605	0.308
24	$(CH_2)_2NEt_2$	H	Me	0.618	0.901
25	$(CH_2)_2NH(CH_2)_2OH$	*n*-BuO	H	0.646	0.339
26	$(CH_2)_2NEt_2$	EtO	H	0.790	0.114
27	$(CH_2)_2NEt_2$	Me	H	0.863	0.786
28	$(CH_2)_2NEt_2$	H	$(CH_2)_2NEt_2$	0.877	0.788
29	$(CH_2)_2NEt_2$	Me_2N	H	0.896	0.317
30	$(CH_2)_2NEt_2$	*n*-BuO	H	1.180	0.073
31	$(CH_2)_3NEt_2$	MeO	H	1.330	0.764
32	$(CH_2)_2NEt_2$	$MeSO_2$	H	1.830	0.774
33	$(CH_2)_2NEt_2$	$PhCH_2O$	H	2.680	1.140
34	$(CH_2)_2NH(CH_2)_2OH$	H	$CH_2CH{=}CH_2$	2.710	1.220
35	Me	H	H	10.000[b]	
36	$(CH_2)_2OH$	MeO	H	10.000[b]	10.000[b]
37	$CH{=}CH_2$	H	Me	10.000[b]	
38	$(CH_2)_2OH$	H	H	10.000[b]	

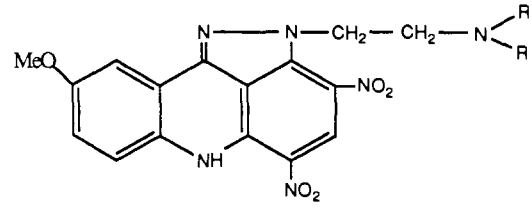

compd	R	IC_{50} (μM)[a] L1210	IC_{50} (μM)[a] HCT-8
39	Me	0.049	0.015
40	Et	0.399	0.066

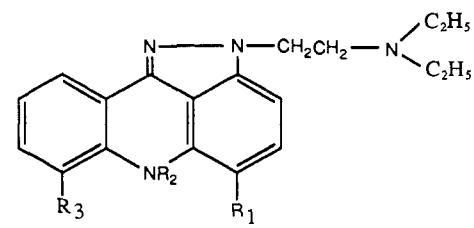

compd	R_1	R_2	R_3	IC_{50} (μM)[a] L1210	IC_{50} (μM)[a] HCT-8
41	$NHCOCH_3$	H	H	10.000[b]	
42	$N{=}CHNMe_2$	Me	H	0.785	0.297
43	NH_2	Me	H	10.000[b]	1.560
44	NO_2	H	MeO	0.645	0.506

[a] Amount of drug required to decrease final cell counts to 50% of the untreated control values. [b] Activity > 1×10^{-5} M.

such as amsacrine and mitoxantrone, pyrazoloacridines cause protein-associated, single- and double-strand breaks in DNA.[3b] The frequency of single- and double-strand breaks correlated with cytotoxicity in L1210 cells, as did the double-strand: single-strand break ratio.

It was suggested that the pyrazoloacridines may have two unrelated mechanisms of action:[3] their in vitro activity against L1210 leukemia, which, incidentally, corresponds well with recent results of in vivo studies against P388 leukemia,[4] is related to protein-associated DNA breaks and may be mediated by DNA topoisomerase II. Other members of the series, which failed to manifest high-potency L1210 cytotoxicity, are, however, active against solid tumors, but at higher concentrations. Additional evidence for two subclasses of pyrazoloacridines with different biochemical mechanisms derived from studies of the inhibition of RNA and DNA syntheses.[1a]

The selectivity of the pyrazoloacridines against solid-tumor cells is notable in light of evidence that cytotoxic anticancer drugs of clinical utility in the treatment of various leukemias and lymphomas have, in general, been rather ineffective against solid tumors such as colon adenocarcinoma, non-small-cell lung cancers, and gastric and pancreatic carcinomas. The variation of in vitro activity shown by these analogues against the human HCT-8 vis-à-vis murine L1210 cell lines offered the opportunity to determine the structural basis for solid-tumor selectivity.

A number of methods have been described to predict novel biologically active compounds on the basis of previously synthesized and tested compounds.[5] Since its introduction in 1988, comparative molecular field analysis (CoMFA)[6a] has produced excellent correlations with enzyme and receptor data[6a-d,f] when utilized as a means to determine three-dimensional quantitative structure–activity relationships (3D-QSAR). The successful extension of CoMFA to results derived from intact biological structures[6e] prompted our interest in the application of the procedure to determine whether the steric and electrostatic properties of the pyrazoloacridines, either alone or together with additional physicochemical parameters (e.g., partition coefficient, log P), can be related to differences within as well as between each set of in vitro cytotoxic data.

Computational Methods

A search of the Cambridge Structural Database at the outset of the present study failed to reveal data for the crystallographic determination of the molecular structure of a single pyrazoloacridine. The 9-methoxy derivative (**15**), an active derivative against HCT-8, was arbitrarily selected as the template molecular model.[7] The structure of the latter and those, as well, of all analogues, each as the free base, were generated with SYBYL version 6.0,[8] option BUILD, running on a Silicon Graphics IRIS (4D/GTX 310) workstation.

The conformational space of the 2-[3-(dimethylamino)propyl] chain attached to the virtually planar polycyclic structure comprising **15** was examined with the random searching algorithm implemented in SYBYL. Local energy minima located for conformations in which the side chain was oriented toward the ring (C) bearing the nitro substituent, were within 2 kcal of corresponding minima of those where in the side chain was arrayed in an opposite direction, i.e., toward ring A. In the absence of any evidence that would reduce the uncertainties regarding biologically active conformations, it appeared reasonable to locate an energy minimum for the template molecular model in which the conformation of the side chain roughly bisected an angle subtended by the two extreme conformations.

Upon completion of the present study, Capps et al.[4] reported the crystallographic analysis of **17** in which the 2-(2-(diethylamino)ethyl) chain is directed toward ring A. However, this recent spectroscopic evidence would not appear to negate the conformation assigned to the template molecule (**15**), considering the relatively small differences ($\ll$2 kcal) in local energy minima associated with the 3D arrangements of the chain.

The side chains of each of the pyrazoloacridines were then oriented as closely as possible to that of **15** and the charges, energies, final geometries of all structures were determined by MOPAC version 6.0[9a] using the AM1[9b] model Hamiltonian. The selection of AM1 as the best semiempirical method for this particular application was confirmed only after the crystallographic data on **17** became available. Thus, the root mean square (RMS) deviations of the solid-state conformation of this analogue from MOPAC geometries, as predicted by MNDO, PM3, and AM1 are 0.961, 0.718, and 0.468, respectively.

Alignment of structures involved rigid-body, RMS-fitting of carbon atoms 5a, 6a, 10a, 10c of each analogue to the corresponding atoms of **15**. An alternative strategy of alignment, steric and electrostatic alignment (SEAL),[10] which optimizes the alignment of three-dimensional structures using their atomic partial charges and steric volumes as factors in combination with a Monte Carlo search procedure, was utilized to provide a comparison of statistical data generated with the RMS alignment.

CoMFA was performed with the QSAR option of SYBYL. The requisite three-dimensional lattice, with 2-Å spacings in the x, y, and z directions, generated automatically by the software, was utilized with both the SEAL and RMS alignments. This grid region overlapped all entered molecules and extended beyond their volumes by at least 4 Å along all axes. The statistical findings derived from L1210 and HCT-8 data were then compared to results obtained, using both methods of alignment and a grid region of the same size, but with spacings of 1 Å. Steric and electrostatic interactions at lattice intersections of both grids were generated with a probe atom that had the van der Waals properties of sp^3 carbon and a charge of +1.0.

The linear expression of the CoMFA results was calculated with the partial least-squares analysis (PLS) algorithm in conjunction with the cross-validation procedure. The calculation provides (inter alia) a determination of the optimal number of components, i.e., that which yields the optimally predictive model as indicated by the highest correlation (predictive r^2) value. PLS analysis of the descriptors with the same number of components but without cross-validation, afforded conventional r^2 values.

Chemistry and Biological Data

The syntheses of all the pyrazoloacridines employed in this study (Table I) have been reported previously.[1b] Likewise, the results of in vitro assays of **1–3** as growth inhibitors of L1210 and HCT-8 cells, which are reproduced in Table I, were disclosed in earlier publications.[2a,b]

Results

Molecular alignment is recognized as the most important determinant of success in a CoMFA study.[6a] Indeed, a low cross-validated r^2 value[11] may indicate a misaligned compound. Accordingly, we sought validation of CoMFA data derived via RMS-fit (see below), using an alternative strategy of alignment. Key considerations in the decision to use SEAL include the fact that, in contrast to RMS fit, no preassigned atom–atom alignments are specified by the user. Therefore, counterintuitive alignments are not ignored. Also, the method is automatic and exhaustive, precluding thereby, the possibility of missed alignments.

The CoMFA-derived QSARs for L1210 and HCT-8, respectively, are summarized in Tables II and III. A comparison of the data indicates that with lattice spacings of 2.0 Å the RMS fit alignment produced somewhat better cross-validated r^2 values for both cell lines than those generated with the SEAL method. It is apparent that the latter afforded r^2 values approaching those obtained with

Table II. Comparison of CoMFA Statistics on L1210 and HCT-8[a]

spacing, Å	offset, Å			L1210		HCT-8	
	X	Y	Z	cross-validated r^2	conventional r^2	cross-validated r^2	conventional r^2
2	0.0	0.0	0.0	0.578	0.939	0.518	0.916
2	1.0	0.0	0.0	0.559	0.942	0.463	0.920
2	0.0	1.0	0.0	0.595	0.941	0.429	0.919
2	0.0	0.0	1.0	0.465	0.931	0.451	0.911
1	0.0	0.0	0.0	0.623	0.952	0.537	0.935
1	0.5	0.0	0.0	0.652	0.956	0.570	0.942
1	0.0	0.5	0.0	0.626	0.963	0.532	0.936
1	0.0	0.0	0.5	0.659	0.960	0.576	0.952

[a] Root mean square alignment.

Table III. Comparison of CoMFA Statistics on L1210 and HCT-8[a]

α	cross-validated r^2			
	L1210		HCT-8	
	2 Å	1 Å	2 Å	1 Å
0.600	0.511	0.559	0.409	0.437
0.550	0.526	0.561	0.409	0.436
0.525	0.538	0.566	0.419	0.440
0.500	0.545	0.570	0.418	0.437
0.475	0.548	0.609	0.403	0.454
0.470	0.548	0.611	0.400	0.456
0.460	0.547	0.612	0.294	0.459
0.450	0.540	0.578	0.374	0.443
0.400	0.487	0.574	0.327	0.450
0.300	0.443		0.357	
0.200	0.393	0.468	0.272	0.337

[a] SEAL alignment.

the RMS fit, but only with the alignment function parameter α of SEAL set at values of 0.470 and 0.525 (2-Å lattice spacings) for the analysis of the L1210 and HCT-8 data, respectively.

Cramer and co-workers noted that large changes in lattice spacings impacted on the final CoMFA results.[6a] Nonetheless, their cross-validated r^2 values indicated that a spacing of 2 Å between lattice points was a good choice for steroid molecules. By contrast, Tables II and III show that with either method of alignment, a large change in lattice spacing, e.g., 2 to 1 Å, causes significant variations in the CoMFA results. A shift in the lattice of half of its spacing had a much smaller effect on the CoMFA data for a lattice of 1 Å than one of 2 Å (Table II). Again, the cross-validated r^2 values obtained with the SEAL method approach those derived with the RMS alignment, but only with optimum values for α. In any case, the reduced spacing between lattice points would seem to be appropriate for the pyrazoloacridines. However, it is important to note that the reduction required a 40–60-fold increase in total computational time to obtain the CoMFA results.

From Table II it is evident that the CoMFA-derived QSARs manifested good cross-validated r^2 and indicating thereby a considerable predictive and correlative capacity for growth inhibition of both the leukemia and solid tumor data. The relative contributions of the steric and electrostatic fields to both QSAR models were about equal. Indeed, elimination of either term from models for the QSAR of L1210 or HCT-8 decreased the cross-validated r^2 for both (data not shown). Inclusion of frontier orbital (HOMO and/or LUMO) energies decreased the significance of the model (data not shown).

It would be expected that the cytotoxicities of the pyrazoloacridines should be influenced by their pharmacokinetic parameters, i.e., transport and distribution, in addition to effects occurring as a consequence of drug–receptor interactions. However, regression analyses of partition coefficients for the pyrazoloacridines in the form of calculated log P values,[12] a measure of relative lipophilicity that is associated with transport and distribution, vs corresponding log(1/IC_{50}) failed to show a correlation in either cell line (L1210, $r^2 = -0.108$; HCT-8, $r^2 = -0.122$). Moreover, the inclusion of log P in CoMFA calculations, understandably, decreased the significance of the model.

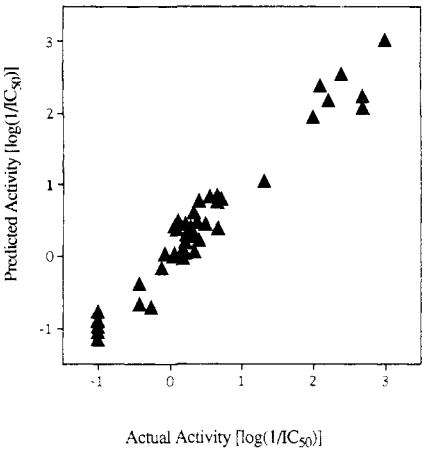

Figure 1. Predicted vs actual growth inhibition (IC_{50}, μM) of L1210 leukemia cells by pyrazoloacridine structures **1–44**.

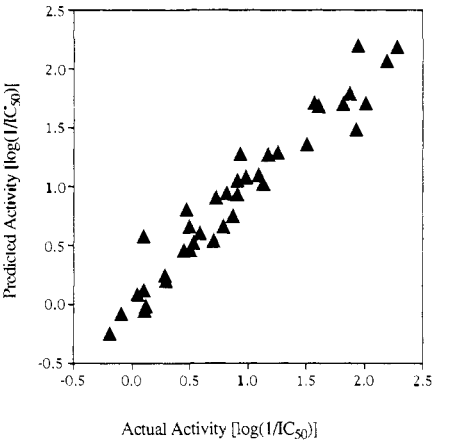

Figure 2. Predicted vs actual growth inhibition (IC_{50}, μM) of HCT-8 cells by pyrazoloacridine structures **1–32, 34, 39, 40,** and **42–44**.

Evidence for the predictive performance of the CoMFA-derived models is provided in Figures 1 and 2 which show plots of actual versus predicted growth inhibition [log(1/IC_{50})] by the pyrazoloacridines of L1210 (44 compounds) and HCT-8 (38 compounds), respectively. The potencies of the pyrazoloacridines against the two cell lines are predicted surprisingly well by models which, in the absence of experimental evidence, were based on hypothetical alignment.

The major steric and electrostatic features of the QSAR are represented in Figures 3 and 4 in the form of three-dimensional contour maps, displayed as semitransparent, shaded surfaces. The surfaces at the top of Figure 3 indicate areas in space around the template molecule (**15**) where increases (yellow region) and/or decreases (cyan region) in steric bulk would enhance growth inhibition of L1210. Surprisingly, essentially the same changes in steric interactions are indicated (at the bottom of this same Figure) to promote growth inhibition of HCT-8 cells. Contour maps of the electrostatic field contributions provided a similar set of results. Thus, the surfaces in

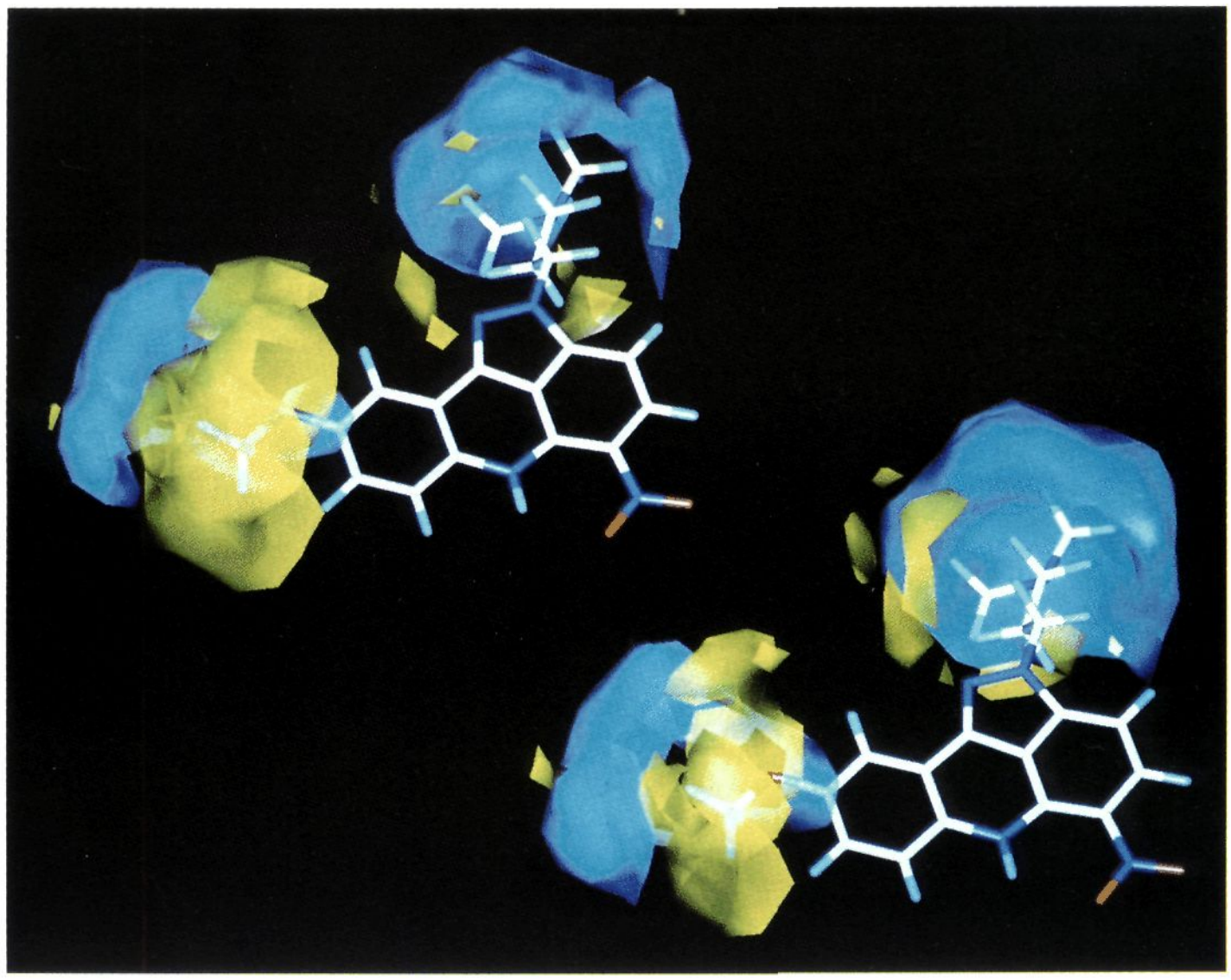

Figure 3. Overlay of structure **15** and steric CoMFA maps (upper left, L1210; lower right, HCT-8). Yellow contours (level –0.003) surround regions where increases in steric bulk would enhance growth inhibition. Cyan contours (level +0.003) encompass regions where decreases in steric interactions would improve growth inhibition.

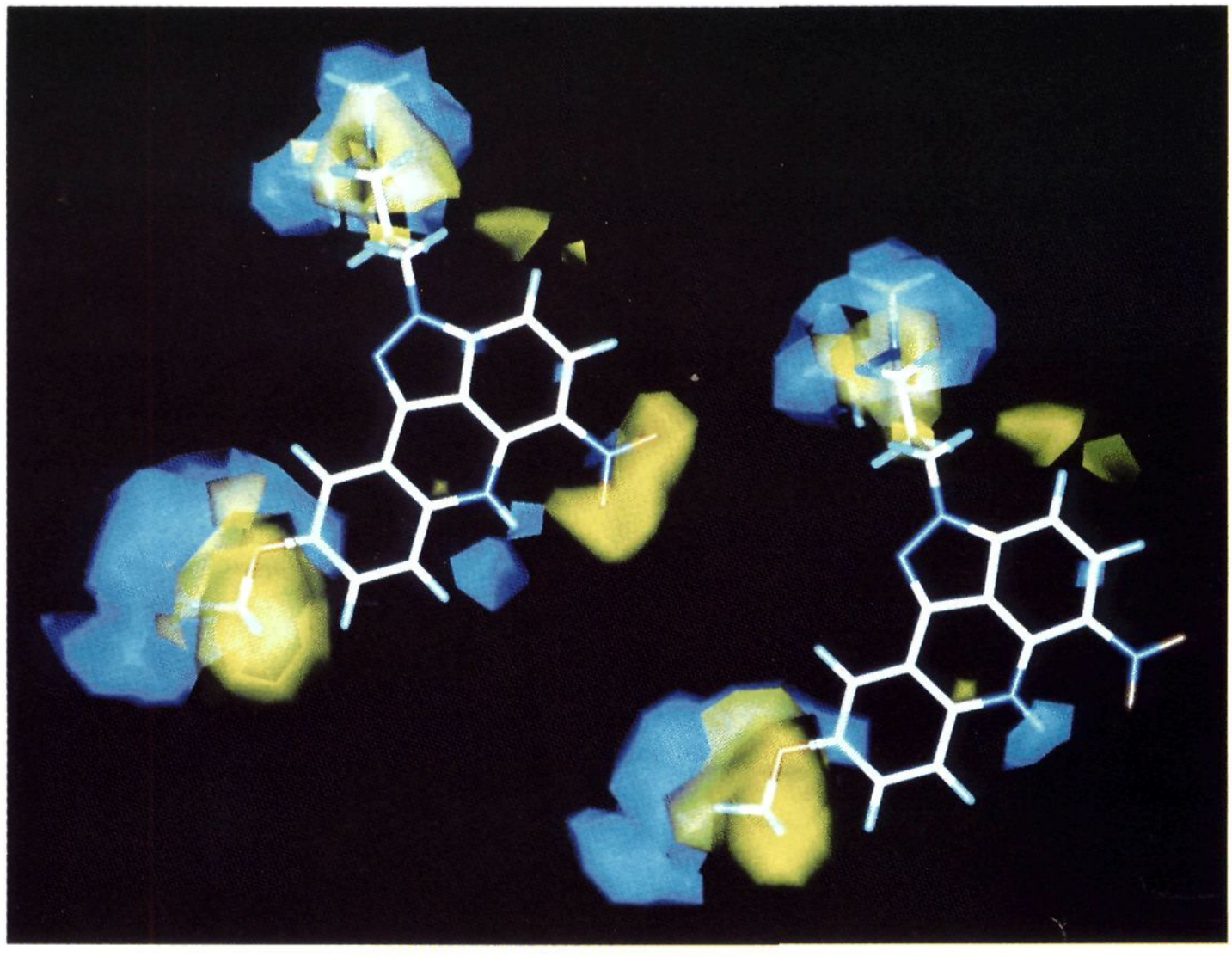

Figure 4. Overlay of structure **15** and electrostatic CoMFA maps, displayed as indicated in legend to Figure 3. Yellow contours encompass regions where a more negative electrostatic interaction would improve growth inhibition. Cyan contours surround regions of positive electrostatic interaction would enhance growth inhibition. Levels are as indicated in Figure 3.

Figure 4 indicate common spatial areas where modifications in **15**, leading to increases or decreases in electrostatic potential, would be favorable to growth inhibition of both L1210 (top) and HCT-8 (bottom) cell lines.

Conclusions

The detailed modeling of the anticancer activities of the pyrazoloacridines presented in the previous section provides the basis for some speculation regarding structure/property correlations. Firstly, the predictive utility of the respective CoMFA-derived models is evident in the good results of Figures 1 and 2. Surprisingly, neither calculated log P, which complements CoMFA descriptors by correlating with the phenomena of transport and distribution (pharmacokinetics), nor HOMO and/or LUMO energies, that reflect the transition state of donor–receptor interactions, contribute to the model. Clearly, the steric and electrostatic fields of the pyrazoloacridines are the sole relevant descriptors to the structure–activity (cross-validated and conventional) correlations obtained with the cytotoxic data for both the L1210 and HCT-8 cell lines. Indeed, the pertinence of these explanatory properties to the correlations of both sets of biological data is manifest in the coefficient contour maps (Figures 3 and 4). It was, however, surprising to find that modifications in the pyrazoloacridines, leading to increases or decreases in electrostatic as well as steric interactions that enhance or are, simply, unfavorable to growth inhibition of L1210 cells have corresponding effects on HCT-8 cells. Thus, for reasons that are not apparent, the physical parameters that comprise CoMFA are inadequate to characterize in the vitro solid tumor selectivity of the pyrazoloacridines. This points to a need to supplement the cytotoxic data of the CoMFA with results of further study that focuses on a quantitative comparison of the potential for differential metabolic activation of the pyrazoloacridines in the two cell lines. The proposed study might explain why **12**, **15**, **17**, and **40**, each of which includes an alkoxy group at the 9-position, are solid-tumor selective,[2] whereas the corresponding hydroxy derivative, **2**, is more cytotoxic (more potent) but not solid-tumor selective in either the Sebolt or Wozniak assay. Thus, it is distinctly possible that O-demethylation may occur more efficiently in cells of solid tumors than in either leukemia or normal cells.

Acknowledgment. The investigation was supported in part by a Program Project Research Grant, CA 46560, from the National Cancer Institute.

References

(1) (a) Sebolt, J. S.; Scavone, S. V.; Pister, C. D.; Hamelehle, K. L.; Von Hoff, D. D.; Jackson, R. C. Pyrazoloacridines, a New Class of Anticancer Agents with Selectivity against Solid Tumors. *Cancer Res.* **1987**, *47*, 4299–4304. (b) Capps, D.; Kesten, S. R.; Shillis, J.; Plowman, J. 2-Aminoalkyl-5-nitropyrazolo[3,4,5-*kl*]acridines. A New Class of Anticancer Agents. *Proc. Am. Assoc. Cancer Res.* **1986**, *27*, 277.

(2) LoRusso, P.; Wozniak, A. J.; Polin, L.; Capps, D.; Leopold, W. R.; Werbel, L. M.; Biernat, L.; Dan, M.; Corbett, T. H. Antitumor Efficacy of PD 115934 (NSC 366140) against Solid Tumors of Mice. *Cancer Res.* **1990**, *50*, 4900–4905.

(3) (a) Jackson, R. C.; Sebolt, J. S.; Shillis, J.; Leopold, W. R. The Pyrazoloacridines: Approaches to the Development of a Carcinoma-Selective Cytotoxic Agent. *Cancer Invest.* **1990**, *8*, 39–47. (b) Sebolt-Leopold, J. S.; Scavone, S. Biochemistry of the Interactions Between DNA and the Pyrazoloacridines, A Series of Biologically Novel Anticancer Agents. *Proc. Am. Assoc. Cancer Res.* **1991**, *32*, 334.

(4) Capps, D. B.; Dunbar, J.; Kesten, S. R.; Shillis, J.; Werbel, L. M.; Plowman, J.; Ward, D. L. 2-(Aminoalkyl)-5-nitro[3,4,5-*kl*]acridines, a New Class of Anticancer Agents. *J. Med. Chem.* **1992**, *35*, 4770–4778.

(5) Marshall, G. R.; Motoc, I. Approaches to the Conformation of the Drug Bound to the Receptor. In *Molecular Graphics and Drug Design*; Burgen, A. S. V., Roberts, G. C. K., Tute, M. S., Eds.; Elsevier Sci. Publ.: Amsterdam, 1986; pp 116–156. Marshall, G. R. Computer Aided Drug Design. *Annu. Rev. Pharmac. Toxicol.* **1987**, *27*, 193–213. Marshall, G. R. Computer-Aided Drug Design. In *Computer-Aided Molecular Design*; Richards, W. G., Ed.; VCH Publishers, Inc.: New York, 1989; pp 91–104. Cohen, N. C.; Blaney, J. M.; Humblet, C.; Grund, P.; Barry, D. C. Molecular Modeling Software and Methods for Medicinal Chemistry. *J. Med. Chem.* **1990**, *33*, 883–894. Dean, P. M. *Molecular Foundations of Drug-Receptor Interaction*; Cambridge Univ. Press: Cambridge, 1987. Fruehbeis, H.; Klein, R.; Wallmeier, H. Computer-Assisted Molecular Design (CAMD)-an Overview. *Angew. Chem., Int. Ed. Engl.* **1987**, *26*, 403–418.

(6) (a) Cramer, R. D.; Patterson, D. E.; Bunce, J. D. Comparative Molecular Field Analysis (CoMFA). 1. Effect of Shape on Binding of Steroids to Carrier Proteins. *J. Am. Chem. Soc.* **1988**, *110*, 5959–5967. Recent applications of the CoMFA approach to structure-activity correlation include: (b) Björkroth, J.-P.; Pakkanen, T. A.; Lindroos, J.; Pohjala, E.; Hanhijärvi, H.; Lauren, L.; Hannuniemi, R.; Juhakoshi, A.; Kippo, K.; Kleimola, T. Comparative Molecular Field Analysis of Some Clodronic Acid Esters. *J. Med. Chem.* **1991**, *34*, 2338–2343. (c) Carroll, F. I.; Gao, Y.; Rahman, M. A.; Abraham, P.; Parham, K.; Lewin, A. H.; Boja, J. W.; Kuhar, M. J. Synthesis, Ligand Binding, QSAR, and CoMFA Study of 3β-(p-Substituted phenyl)tropane-2β-carboxylic Acid Methyl Esters. *J. Med. Chem.* **1991**, *34*, 2719–2725. (d) Wiese, T. E.; Palomino, E.; Horwitz, J. P.; Brooks, S. C. Comparative Molecular Field Analysis (CoMFA) of the Specific Responses of MCF-7 Cells to A-Ring Substituted Estrogens. *Abstracts, 201st American Chemical Society National Meeting*, Atlanta, GA, April 14–19, 1991; American Chemical Society, Washington, D.C. 1991; MEDI.150. (e) McFarland, J. W. Comparative Molecular Field Analysis of Anticoccidial Triazines. *J. Med. Chem.* **1992**, *35*, 2543–2550 and additional references cited therein. (f) Waller, C. L.; McKinney, J. D. Comparative Molecular Field Analysis of Polyhalogenated Dibenzo-p-dioxins, Dibenzofurans, and Biphenyls. *J. Med. Chem.* **1992**, *35*, 3660–3666.

(7) A similar rationale in the selection of a reference compound is cited in ref 6e.

(8) Tripos Associates, 1699 S. Hanley Road, Suite 303, St. Louis, MO 63144.

(9) (a) Stewart, J. J. P. MOPAC: A General Molecular Orbital Package (Version 6.0). *Quantum Chemistry Program Exchange Catalogue (QCPE)* **1992**, IV, 19–20. (b) Dewar, M. J. S.; Zoebisch, E. G.; Healy, E. F.; Stewart, J. J. P. AM1: A New General Purpose Quantum Mechanical Molecular Model. *J. Am. Chem. Soc.* **1985**, *107*, 3902–3909.

(10) Kearsley, S. K.; Smith, G. M. An Alternative Method for Alignment of Molecular Structures: Maximizing Electrostatic and Steric Overlap. *Tetrahedron Comput. Methodol.* **1990**, *3*, 615–633.

(11) The level of significance (F) of each r^2 value determined in this study is greater than 99%.

(12) PRO-LOGP, version 4.1E; CompuDrug USA, Inc., P.O. Box 202078, Austin, TX 78720. A comparison of estimated values of log P for several pyrazoloacridines obtained by this program with those derived for corresponding structures via the program CLOGP (DAYLIGHT Chemical Information Systems, Inc.) showed significant differences. However, values obtained by both methods appeared to be self-consistent.